

The Effects of Variable Thermal Conductivity on Mantle Heat-Transfer

Arie P. van den Berg,¹ David A. Yuen,² Volker Steinbach¹

Abstract. We have examined the styles of steady-state convective heat transfer for two kinds of mantle thermal conductivity models in an aspect-ratio one box. We have employed the phonon portion of the thermal conductivity model of Hofmeister (1999) and varied the radiative component in this model. We have also considered a second model which emphasizes radiative heat transfer and has a high contribution in the lower mantle. We have conducted constant viscosity calculations out to a surface Ra of 10^{10} . Variable conductivity enhances in most cases the surface heat flow. The smallest deviation from the constant conductivity model comes from the phonon model with the parameters associated with oxides. Larger heat flow is obtained with silicates and increasing radiative contributions associated with the values of Shankland et al. (1979). The highest heat flow values are obtained for the radiatively dominated model, where the thermal conductivity in the deep mantle can be a factor of 50 greater than the surface conductivity value.

Introduction

Recently a new model of mantle thermal conductivity has been introduced by Hofmeister (1999) based on thermodynamics, lattice dynamics and infra-red spectroscopy. This model of thermal conductivity has both temperature and pressure dependence and has stimulated several studies in mantle convection and geodynamics (Dubuffet et al., 1999; Dubuffet and Yuen, 2000; Starin et al., 2000; Hauck et al., 1999; Branlund et al., 2000). Temperatures are found to be higher (Dubuffet et al., 1999; Hauck et al., 1999) and the planforms of plumes are more focussed (Dubuffet and Yuen, 2000).

However, the important issue of convective heat-transfer with variable conductivity still has not been examined, although both the conductive solutions of Starin et al. (2000) and Hauck et al. (1999) show some non-negligible increase in the temperature of sedimentary basins and slabs. Here we will illustrate the effects of variable k on global heat-transfer in high Rayleigh number convection and delineate the relative importance between the phonon and photon contributions to temperature- and pressure-dependent conductivity $k(T, P)$.

¹Dept. Theoretical Geophysics, Institute of Earth Sciences, Utrecht University, Utrecht, The Netherlands

²Dept. of Geology and Geophysics, Minnesota Supercomputer Institute, University of Minnesota, Minneapolis, USA

Copyright 2001 by the American Geophysical Union.

Paper number 2000GL011903.
0094-8276/01/2000GL011903\$05.00

Technical Description

The thermal conductivity k employed comes from a semi-empirical model calculated from thermodynamic properties and vibrational spectroscopy at ambient conditions (Hofmeister, 1999) and supported by a physical model based on spectroscopy at high temperature T and pressure P conditions. It takes the form

$$k(T, P) = k_0(298/T)^a \exp[-(4\gamma + 1/3)\alpha(T - 298)] \left(1 + \frac{K_0' P}{K_0}\right) + \sum_{i=0}^3 b_i T^i \quad (1)$$

where $k_0 = 4.7WK^{-1}m^{-1}$, temperature T is in Kelvin, the Grueneisen parameter, $\gamma = 1.2$, thermal expansivity $\alpha = 2.0 \times 10^{-5}K^{-1}$, the bulk modulus $K_0 = 261GPa$ and the pressure derivative of the bulk modulus, $K_0' = 5$ (Hofmeister, 1999). The fitting parameter a is 0.9 for oxides and 0.3 to 0.4 for silicates (Hofmeister, 1999). The radiative contribution is given by the coefficients b_i in eqn (1), which is obtained from a least-square fit to the spectroscopic data of the overtones. In the first conductivity model we will use these b_i from Hofmeister (1999). The radiative contribution in this model contributes at most 5 to 7 % to the total conductivity. We will also employ a second conductivity model with an enhanced radiative contribution by increasing the b_i by a factor of 4.7. This augmentation of the radiative component would mimic the radiative contribution proposed by Shankland et al. (1979), which had a k due to radiation of around $0.2WK^{-1}m^{-1}$ at about $2000C$. We will designate eqn (1) the phonon-dominated conductivity model. The viscosity η varies the same with temperature as k , since both $\partial\eta/\partial T$ and $\partial k/\partial T$ are negative. Both η and k will provide positive feedback with each other, since a lower conductivity from an increase of T would trap the heat locally, thus decreasing the local viscosity.

For assessing the effects of a truly radiative conductivity, we have considered a third conductivity in which $\partial k/\partial T$ is constrained to be positive. This is carried out by changing the sign of a in eqn (1) and also changing the minus sign inside the exponential argument in eqn (1) from minus to plus. The b_i come from Hofmeister (1999) model. This third conductivity model is similar in spirit to the effect of grain-size variation on mantle viscosity (Solomatov, 1996, Riedel and Karato, 1997), in which the viscosity could increase with temperature, or $\partial\eta/\partial T > 0$.

We have employed a finite element model based on the primitive variables of u , the velocity, T , the temperature and p the dynamical pressure (van den Berg et al., 1993). The vigor of convection is controlled by the surface Rayleigh number Ra_s , which appears in the momentum equation. The energy equation takes on a different character with $k(T, P)$. For no internal heating and in the Boussinesq ap-

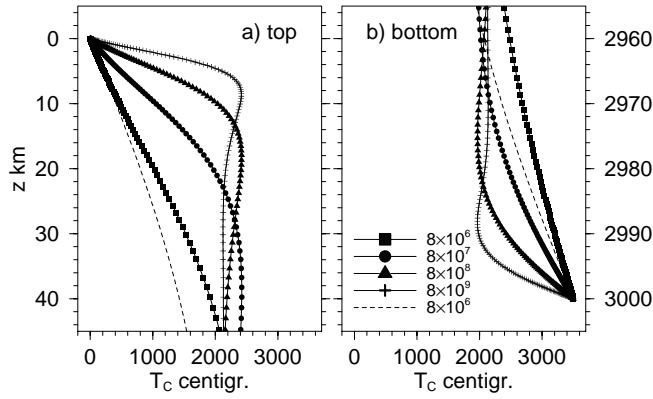


Figure 1. Temperature profiles $T_C(z)$ at mid-point $x = 0.5$ for phonon-dominated conductivity. Surface Rayleigh numbers are 8×10^6 , 8×10^7 , 8×10^8 and 8×10^9 . There is a 3500 degree temperature difference between the surface and the bottom of the mantle. Grids ranging from 300×300 to 500×500 points have been employed. Conductivity parameters values from (Hofmeister, 1999) with $a = 0.3$ are used

proximation this takes the form:

$$\frac{DT}{Dt} = \kappa(T, P)\nabla^2 T + \frac{\partial \kappa}{\partial T}(\nabla T)^2 + \frac{\partial \kappa}{\partial P} \frac{\partial T}{\partial z} \quad (2)$$

where $\kappa(T, P)$ is the variable thermal diffusivity and D/Dt is the substantive derivative. We solve the set of momentum and energy equations with a conservative formulation in the steady-state limit in which $\partial T/\partial t$ is set to zero. This approach allows us to explore rapidly a wide parameter space. We used the Picard-type iterative scheme to solve the system of nonlinear equations involving momentum and energy. We note that the right-hand side of eqn (2) has three nonlinear terms with a strong nonlinearity in T present. As noted already in Dubuffet et al. (1999) many more points are needed for convection with variable thermal conductivity than with constant conductivity. We have used up to 500×500 grid points consisting of linear temperature and quadratic velocity elements, in order to go up to a high Ra_s of 10^{10} . In this aspect-ratio one case, these steady-states can be achieved, albeit at the expense of large computer memory for the direct-solvers of the steady-state finite element equations, requiring a total of 5 Gbytes of program memory. We have set a global convergence criterion of 10^{-2} for both the T and u fields.

Results and Discussion

We have conducted a series of steady-state calculations in an aspect-ratio one box for Ra_s , going up to 8×10^9 for both the phonon-dominated ($\partial k/\partial T < 0$) and the photon-assisted ($\partial k/\partial T > 0$) thermal conductivity models. In a Boussinesq model the interior temperature is nearly constant and we shall focus on the thermal structure at the boundary layers. We take the temperature profile at the mid-point of the box, which is nearly the same as the horizontally averaged temperature profile. We have studied first the effects of $a = 0.3$ in the phonon model. Figure 1 shows the temperature profiles of Ra_s going from 8×10^6 to 8×10^9 for both the top (Fig.1a) and bottom (Fig.1b) boundary layers. We have shown a constant conductivity case ($Ra = 8 \times 10^6$) shown in the dotted curve as a com-

parison. We observe that with variable conductivity the temperature is a couple of hundred degrees hotter than for constant conductivity case, as found previously by Dubuffet et al. (1999) in 3-D geometry. The temperature gradient at the surface is higher for variable conductivity, indicating a greater surface heat flow. The top thermal boundary layers are thinner with variable conductivity, requiring higher numerical resolution. There is an asymmetry in the thermal boundary structure between the top and bottom with a thicker bottom thermal boundary layer, related to the higher averaged conductivity near the bottom boundary.

Fig.2 shows the corresponding results for a phonon model whose radiative component has been enhanced by a factor of 4.7 to make it more like the one proposed by Shankland et al. (1979). The same range of Ra_s as in Fig.1 has been explored. The thermal boundary layers are thinner resulting in higher temperatures by several hundred degrees in the top boundary layer mainly at the lower Ra_s .

The thermal conductivity profiles for both the regular radiative and the enhanced radiative (Shankland et al., 1979) models are shown in Fig. 3. The conductivity profiles are embedded within the thermal boundary layers. There are finer features near the top for the enhanced radiative model. A narrow zone at high Ra_s with a width of a km in the enhanced radiative case in Fig. 3b illustrates the need for a high resolution grid in order to resolve the physics. We used 500×500 points and grid refinement in the boundary layers, with a minimum spacing of $37.5m$. Away from the thermal boundary layers the conductivity profiles increase linearly with depth due to the pressure dependence. The conductivity variations at the base of the mantle are less severe than the variations near the surface. The asymmetry with lower conductivity values in the top boundary layer is reflected in the similar asymmetry with higher $\partial T/\partial z$ near the top, shown in Fig.2.

The third thermal conductivity we have considered is strictly radiative, because $\partial k/\partial T$ is positive. There are dramatic differences in the thermal conductivity values between the two phonon models and this photon model, with the photon thermal conductivity being much greater than the phonon models. The values of the photon k in the deep mantle approach values greater than $100 W/Km$, close to gold and platinum. In spite of the averaged Ra being re-

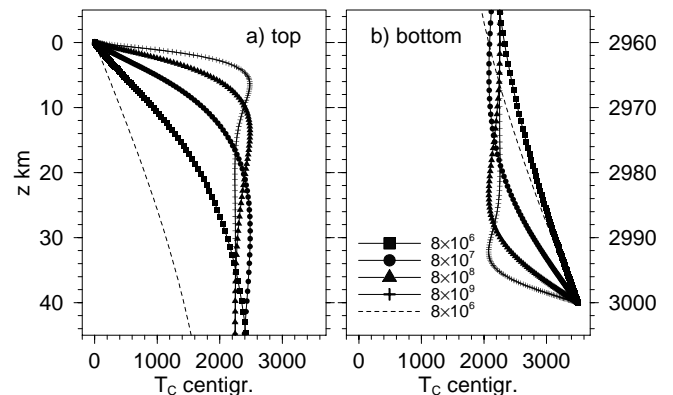


Figure 2. Temperature profiles at mid-point for radiation enhanced conductivity. Radiative conductivity has been enhanced by a factor $f = 4.7$ compared to Fig.1.

duced by two orders in magnitude by the photon conductivity, the highest surface heatflow takes place for the photon model. This interesting result is displayed in Fig. 4, where the surface heat flow is plotted against Ra_s for the constant conductivity, the photon model ($a = -1.0$ and a positive exponential argument), two phonon models with $a = 0.3$ and two radiative factors $f = 1.0$ (Hofmeister, 1999) and $f = 4.7$ (Shankland et al., 1979), a phonon model with $a = 1.0$ and $f = 1.0$ and a model with an averaged thermal conductivity taken from $a = 0.3$ and $f = 4.7$. We have verified our constant conductivity results with those taken from Christensen (1989).

The surface heat flow is the smallest for the phonon model with ($a = 0.3, f = 1.0$) and the constant conductivity model with the enhanced radiative models ($f = 4.7$) (Shankland et al., 1979) and photon models ($a = -1$) lying above it. The effect of a smaller a ($a = 0.3$) combined with ($f = 4.7$) is to increase the heat transfer by a factor of 2 over those for constant conductivity. This increase is related to a similar increase of k in the bottom boundary layer shown in Fig.3. The great sensitivity of heat-transfer to the sign of $\partial K/\partial T$ is revealed by the top line ($\partial K/\partial T > 0$, radiatively dominated) to the other curves with $a > 0$ and $\partial K/\partial T < 0$.

Our results for heat-transfer scaling with the surface Rayleigh number have quite a profound impact on parameterized thermal history (e.g. Sharpe and Peltier, 1978), as this shows quite evidently the importance of variable thermal conductivity. It is clearly obvious that photon mode of conductivity increases the surface heat flow.

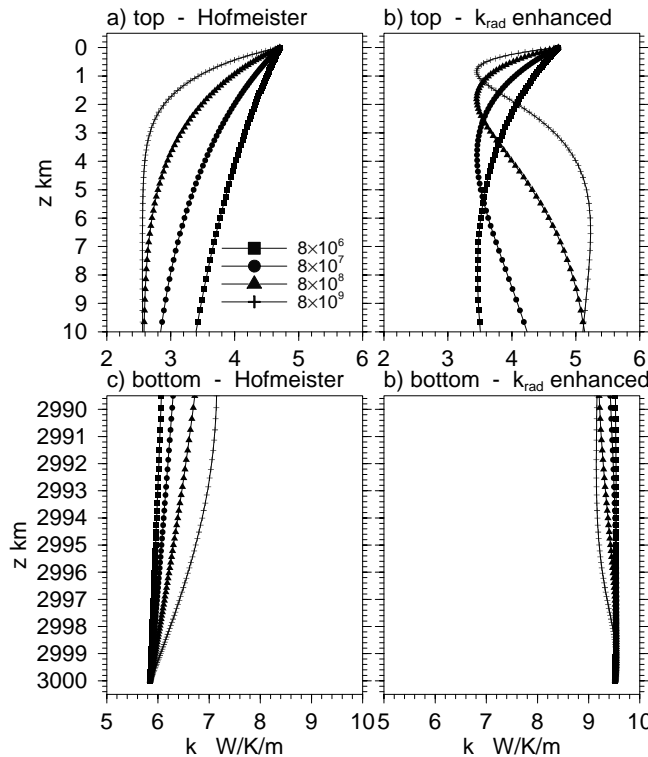


Figure 3. Thermal conductivity profiles at mid-point for the models shown in Fig.1 and 2. Panels (a) and (c) display the top and bottom portions of the conductivity model from (Hofmeister, 1999) while panels (b) and (d) portray the top and bottom portions of the model with enhanced radiative conductivity.

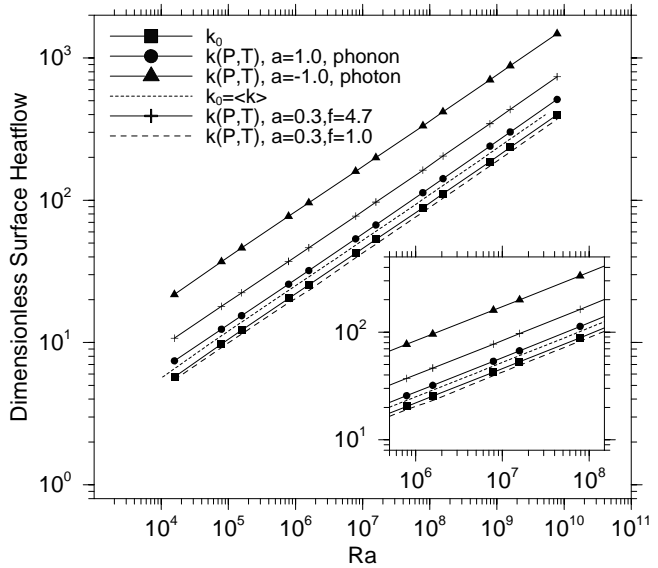


Figure 4. Surface heat-flow versus Ra_s for constant and variable conductivity models. The heatflow scale value is $5.48mWm^{-2}$. a) The solid squares denote constant conductivity results. b) The dashed line represents the results of the (Hofmeister, 1999) model and ($a = 0.3$). c) The pluses show the results for the model with enhanced radiative conductivity and ($a = 0.3$). d) The dotted line shows results for the uniform conductivity case where values of Ra have been reduced by $1/\langle k \rangle$, where $\langle k \rangle$ is the average conductivity of the corresponding run of case c). e) The bullets are for a model as in c) but with $a = 1.0$ and f) the triangles denote a case as in c) with $a = -1$ (photon conductivity). Inset shows a zoom-in of the six cases in a range of geophysical interest.

If the lower mantle thermal conductivity were really radiative in character (Mac Donald, 1959) ($a = -1.0$), there would be much greater heat loss than in the phonon-dominated model (Hofmeister, 1999). The planet would cool very fast in this case and some sort of layered convection enforced by phase transitions at high Ra (Yuen et al., 1995) would be required to produce an acceptable cooling rate. These results also call to question the sole important role accorded to variable viscosity in mantle convection, since there will be tradeoff coming from the nonlinear interaction between variable viscosity and variable conductivity, which makes the usual argument of Ra proportional to $1/\eta(T)$ not valid, since the term $1/k(T)$ also appears in Ra .

Depending on the spatial distribution of the the dominant mode of heat conduction, the interaction of variable conductivity with a grain-size sensitive rheology (Solomatov, 1996) would also cause very different evolutionary paths in thermal evolution. This is due to the fact that both positive and negative feedbacks are possible, depending on the signs of $\partial k/\partial T$ and $\partial \eta/\partial T$. Positive feedback would resonate when both $\partial k/\partial T$ and $\partial \eta/\partial T$ have the same sign, while negative feedback would occur, when $\partial k/\partial T$ has an opposite sign to $\partial \eta/\partial T$.

Acknowledgments. We thank Anne Hofmeister, Fabien Dubuffet, and Tommy Nakakuki for stimulating discussions and M.C. Kameyama and an anonymous reviewer for a conscientious review. This research has been supported by Dutch NWO organization and the geophysics program of the National Science Foundation.

References

- Branlund, J., M.C. Kameyama, D.A. Yuen and Y. Kaneda, Effects of temperature-dependent thermal diffusivity on shear instability in a viscoelastic zone: Implications for faster ductile faulting and earthquakes in the spinel stability field, *Earth Planet. Sci. Lett.*, *182/2*, 2, 171-185, 2000.
- Christensen, U.R., The heat transport by convection rolls with free boundaries at high Rayleigh number, *Geophys. Astrophys. Fluid Dyn.*, *46*, 93-103, 1989.
- Dubuffet, F., Yuen, D.A. and M. Rabinowicz, Effects of a realistic mantle thermal conductivity on the patterns of 3-D convection, *Earth Planet. Sci. Lett.*, *171*, 401-409, 1999.
- Dubuffet, F. and D.A. Yuen, A thick pipe-like heat-transfer mechanism in the mantle: nonlinear coupling between 3-D convection and variable thermal conductivity, *Geophys. Res. Lett.*, *27*, No. 1, 17-20, 2000.
- Fowler, A.C., On the thermal state of the Earth's mantle, *J. Geophys.* *53*, 42-51, 1983.
- Hauck, S.A., R.J. Phillips, and A.M. Hofmeister, Variable conductivity: Effects on the thermal structure of subducting slabs, *Geophys. Res. Lett.*, *26*, No. 2, 3257-3260, 1999.
- Hofmeister, A.M., Mantle values of thermal conductivity and the geotherm from phonon lifetimes, *Science*, *283*, 1699-1706, 1999.
- Mac Donald, G.J.F., Calculations on the thermal history of the earth, *J. Geophys. Res.*, *64*, 1967-2000, 1959.
- Riedel, M.R. and S. Karato, Grain-size evolution in subducted oceanic lithosphere associated with the olivine-spinel transformation and its effects on rheology, *Earth Planet. Sci. Lett.*, *148*, 27-44, 1997.
- Shankland, T. J., U. Nitsan, and A. G. Duba, Optical absorption and radiative heat transport in olivine at high temperature, *J. Geophys. Res.*, *84* No. B4, 1603-1610, 1979.
- Sharpe, H.N. and W.R. Peltier, Parameterized mantle convection and the Earth's thermal history, *Geophys. Res. Lett.*, *5*, 737-740, 1978.
- Solomatov, V.S., Can hotter mantle have a larger viscosity? *Geophys. Res. Lett.*, *23* 9, 937-940, 1996.
- Starin, L., D.A. Yuen, and S.Y. Bergeron, Thermal Evolution of Sedimentary Basin Formation with Temperature-Dependent Conductivity, *Geophys. Res. Lett.*, *27*, No. 02, 265-268, 2000.
- van den Berg, A. P., P.E. van Keken, and D.A. Yuen, The effects of a composite non-Newtonian and Newtonian rheology on mantle convection, *Geophys. J. Int.*, *115*, 62-78, 1993.
- Yuen, D.A., S. Balachandar, V. Steinbach, S. Honda, D.M. Reuteler, J.J. Smedsmo and G.S. Lauer, Non-equilibrium effects of core cooling and time-dependent internal heating on mantle flush events, *Non-linear Processes in Geophysics*, *2*, 206-221, 1995.

A. van den Berg and V. Steinbach, Dept. of Theoretical Geophysics, Institute of Earth Sciences, Utrecht University, 3508 TA Utrecht, Netherlands. (e-mail: berg@geo.uu.nl; steiney@geo.uu.nl)

D. Yuen, Dept. of Geology and Geophysics, Minnesota super-computer Institute, University of Minnesota, Minneapolis, MN 55415-1227, USA. (e-mail: davey@msi.umn.edu)

(Received June 16, 2000; revised November 15, 2000; accepted November 27, 2000.)